Theoretical Investigation of the Photochemical C^2-C^6 Cyclisation of Enyne–Heteroallenes

Carsten Spöler[b] and Bernd Engels*[a]

Abstract: Herein we discuss computations that explain experimental results regarding a highly efficient triplet analogue of the C^2-C^6 cyclisation of enyne–heteroallenes recently discovered by Schmittel and co-workers.[1] To shed some light on the reasons for the differences found between enyne–carbodiimides, enyne–ketenimines and enyne–allenes, we have computed the reaction profiles of the C^2-C^6 and of the C^2-C^7 cyclisations for various model compounds, assuming that the reactions take place on the lowest-lying triplet surfaces. Our results nicely explain the differences and the unexpected high efficiency found for the enyne–carbodiimides. The differences between enyne–carbodiimides and enyne–ketenimines prove to be due to differences in the shapes of the corresponding triplet surfaces. In contrast to the enyne–carbodiimides, for which our calculations predict that a direct cyclisation to the biradical intermediates should occur after the vertical excitation, the enyne–ketenimines relax into a local minimum on the triplet surface. As a consequence, further reaction channels are opened. Our computations indicate that enyne–allene compounds do not react because the necessary excitation energy lies outside the range of the employed triplet photosensitizer. Finally, the close agreement between our results and the experimental findings indicates that the underlying reasons for the differences in the photochemical behaviour of enyne–carbodiimides, enyne–ketenimines and enyne–allenes are related to differences in the electronic structures of the parent systems, while substituent effects are less important.

Keywords: computer chemistry · cyclisation · photochemistry · enyne–heteroallenes

Introduction

Thermal cyclisations of enediynes,[2–4] enyne–allenes[5–10] and their hetero analogues[11] (Scheme 1) have aroused great interest for theory[3, 4, 9–11] and synthesis[2, 5–8, 11, 12] over the last two decades, since these cycloaromatisations constitute the key steps in the synthesis of highly potent antitumour antibiotics.[12, 13]

The thermal cyclisations of enyne–allenes were first investigated by Myers et al.[5] and independently by Saito and co-workers.[6] They showed that the C^2-C^7 cyclisation of enyne–allenes (Myers–Saito cyclisation) leads to α,3-didehydrotoluene biradicals. Control over the regioselectivity of cyclisation reactions of enyne–allenes was first developed by

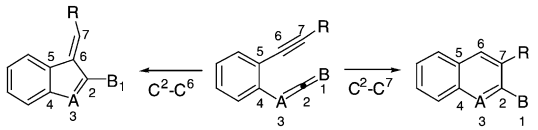

A=CH, N; B=CR'R'', NR'

Scheme 1. Thermal cyclisation reactions of enyne–allenes and their hetero analogues.

Schmittel et al.,[7] who showed that an appropriate choice of substituents at the alkyne terminus allows the regioselectivity of thermal enyne (hetero)-allene biradical cyclisations to be steered away from the Myers–Saito and towards a C^2-C^6 cyclisation pathway, leading to (hetero)-benzofulvene compounds (Scheme 1). Theoretical investigations revealed that the mechanism of the thermal C^2-C^6 cyclisation strongly depends on the substituent at the alkyne terminus.[9a, 9e] For phenyl as substituent, the reaction proceeds through biradical intermediates. Both for π-donor substituents such as NH_2 and for strongly electron-withdrawing substituents such as NO_2, computations predict carbene-like intermediates. Although the mechanism is the same for both types of substituent, the reasons are different.[9d] Besides these mechanisms, computations[9d] also predicted that for the bulky substituent *t*Bu the free activation energy values ($\Delta G^{\neq}$) for the biradical and for

[a] Prof. Dr. B. Engels
Institut für Organische Chemie
Universität Würzburg, Am Hubland
97074 Würzburg (Germany)
Fax: (+49) 931-8884606
E-mail: bernd@chemie.uni-wuerzburg.de

[b] Dipl.-Chem. C. Spöler
Stranski-Lab., Secretariat TC 7
Technical University of Berlin
Strasse des 17. Juni 124, 10623 Berlin (Germany)

DOI: 10.1002/chem.200305001

the ene mechanism differ by less than 1 kcal mol^{-1}, so the ene reaction also has to be taken into account as a mechanistic option for this interesting cyclisation.

As the novel C^2-C^6 cyclisation of enyne–allenes has become the focus of extensive research,[14] the development of a photochemical variant, as found for the Bergman cyclisation,[15] would open a convenient route to the intermediate biradicals of the C^2-C^6 cyclisation. Indeed, Schmittel et al. recently presented a highly efficient photochemical cyclisation of substituted enyne–carbodiimides, with yields higher than 90%.[1] In contrast to the thermal cyclisation, only products of the C^2-C^6 cyclisation are found in the photochemical reactions. To establish the photocyclisation as a general route to triplet heterobenzofulvenes, Schmittel et al. additionally subjected some stable enyne–ketenimines to the same reaction conditions as employed for the enyne–carbodiimides.[1] They found that the cyclisation could also be effected, but that the yields were reduced due to formation of polymeric material. For example, in toluene the conversions are still around 100%, but the yields vary between 50 and 62%. Tests with enyne–allenes showed no reaction at all.[16] To obtain some insight into the mechanism of the photochemical cyclisation, Schmittel et al. systematically varied the energies of the triplet quenchers. The results of these investigations indicate that the cyclisation takes place on the triplet surface. This mechanism is supported by the fact that allenes and heteroallenes are readily excited to triplet states and is in line with the regioselectivity of the reaction, since the regioselective 5-*exo-dig* cyclisation of triplet biradicals is well established.[17]

While it seems clear that the reaction proceeds through the lowest-lying triplet state, some puzzling questions remain. The well established 5-*exo-dig* regioselectivity for triplet biradicals is a general experience, but the underlying reasons for the present case remain unclear; the reasons for the extraordinary yields found for enyne–carbodiimides, for example, are not known and the differences in the yields found for enyne–carbodiimides and those found for enyne–ketenimines or enyne–allenes are still not understood. It is unclear whether this behaviour is a result of the influence of the substituents or of differences in the electronic structures of the parent systems. To address these open questions we performed a theoretical study to investigate whether the experimental data can be explained by the shapes of the lowest-lying triplet surfaces. The study focuses on the different yields found for the various compounds tested in the work of Schmittel et al.[1]

Theoretical Considerations

Our investigations were based on the mechanism indicated in Scheme 2. In the first step the reactant is excited to its lowest-lying triplet state (T_1) by a vertical excitation that happens either directly through energy transfer from the employed triplet quencher or by a fast relaxation out of higher lying singlet electronic states. After the vertical excitation process the molecule is situated on the triplet surface but still possesses the S_0 geometry. This point on the triplet surface is denoted below as $T_1(S_0\,\text{geom})$. While the S_0 geometry

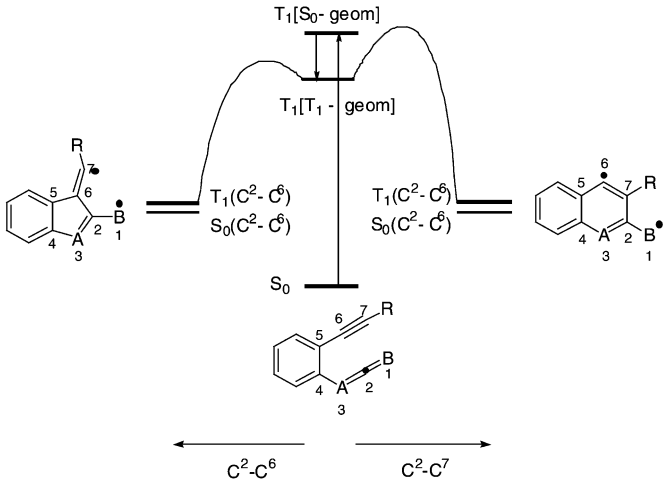

Scheme 2. Assumed mechanism for the photochemical cyclisation of enyne–heteroallenes.

represents a minimum on the ground-state surface it is not normally a stationary point for the triplet surface. As a result of the non-vanishing energy gradients, and depending on the shape of the potential energy surface (PES) of the triplet state around the S_0 geometry, the molecule may either cyclise without a barrier or relax to a local minimum near to the S_0 geometry. This local minimum of the triplet surface is denoted $T_1(T_1\,\text{geom})$. The natures of the stationary points (minima or transition states) were analysed by computations of the vibrational frequencies.

The cyclisation itself is assumed to take place on the lowest-lying triplet surface. It leads either to the triplet state of the biradical intermediate of the C^2-C^6 cyclisation, referred to below as $T_1(C^2-C^6)$, or to that of the C^2-C^7 cyclisation, which is called $T_1(C^2-C^7)$. After the cyclisation, the molecule may cross to the singlet states of the biradical intermediates—$S_0(C^2-C^6)$ and $S_0(C^2-C^7)$, respectively—from which it reacts to give the product in one or more final steps. In this case the final steps are identical to the final steps of the thermal cyclisations; that is, both the photochemical and the thermal reaction can be expected to proceed along the same reaction course for this later stage of the reaction. If possible reactions of the triplet biradical intermediates are faster than the intersystem crossing (fast intermolecular radical additions or hydrogen abstractions, for example), we may have to take account of consecutive reactions other than those found for the thermal cyclisation reactions.

To estimate the meaningfulness of model computations, relationships between experimentally determined data and single steps of the overall reaction must be discussed. The conversion of the reactants depends on the excitation step itself. The probability of the transition to the triplet state is determined by the position of the triplet state with respect to the ground state, which is in turn strongly influenced by the substitution pattern of the reactant. Furthermore, the nature of the triplet photosensitizer utilised in the reaction is also important. Relative yields of possible products do not mainly depend on the excitation process itself but on the regioselectivity of the cyclisation step, on the intersystem crossing from the T_1 states of the biradical intermediates to the

corresponding S_0 states, and on the final reaction steps leading to the products. If one of these steps takes a long time on this timescale, due to possible hindrances, the yield of the corresponding product will be reduced due to formation of by-products, because all intermediates represent very reactive systems (Scheme 3).

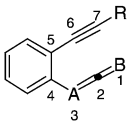

1: A=N, B=NH
2: A=N, B=CH_2
3: A=CH, B=CH_2

Scheme 3. Model compounds employed in this work.

The intersystem crossing will be very efficient, since the lowest T_1 and S_0 states of the biradical intermediates are very close in energy. If the crossing is faster than possible subsequent reactions of the triplet intermediates, the final steps leading to the products are identical to the final steps in the thermal cyclisation. The subsequent steps for the C^2-C^6 cyclisation of enyne–allene systems, which are intramolecular in nature, were found to be so fast that interception of the biradical intermediates failed.[7a] Consequently, for the C^2-C^6 cyclisation we can expect that the relative yield of this photochemical cyclisation course depends only on the cyclisation itself, since the remaining reaction steps are very fast and very efficient. In contrast, the biradical intermediate of the C^2-C^7 cyclisation of enyne–allenes must intercept, and so, unlike in the C^2-C^6 cyclisation, we have to consider intermolecular rather than intramolecular consecutive reactions.

As discussed above, we can assume that the differences in the yields found for enyne–carbodiimides and enyne–ketenimines are connected with alterations in the shapes of the reaction profiles of the cyclisation modes. However, it is unclear whether these differences result from the influence of the substituents or whether differences in the electronic structures of the parent systems are responsible, since the substituents employed in the experimental study for enyne–carbodiimides and for enyne–ketenimines are similar but not identical. Nevertheless, the similarity between the employed substituents leads to the expectation that the alterations mainly arise due to differences in the electronic structures of the parent systems. To shed some light on the open questions we computed the energy profiles for the C^2-C^6 and the C^2-C^7 cyclisation modes for the model compounds **1**–**3** depicted in Scheme 3. Except for the annulated benzene ring, which was present in all of the experimentally employed compounds, in our model systems we replaced all substituents by hydrogen centres to reduce the computational effort. Consequently, substituent effects are not accounted for in our model but, as discussed above, reasons exist which indicate that the differences in the photochemical behaviour arise due to alterations in the electronic structures of the parent systems.

Both cyclisation processes are mainly determined by the following points on the triplet PES. On the assumption of a vertical excitation, the molecule is elevated to the triplet surface with conservation of the geometry of the S_0 ground state ($T_1(S_0\,\text{geom})$). While this arrangement of nuclei is a minimum on the S_0 surface it does not normally represent a stationary point on the triplet PES. Because of the non-vanishing energy gradients, the nuclei start to relax towards the nearest local minimum $T_1(T_1\,\text{geom})$. The energy difference between $T_1(S_0\,\text{geom})$ and $T_1(T_1\,\text{geom})$ represents a lower limit of the excess energy available to overcome possible reaction barriers to the cyclisation modes. The relative reaction rates of both competing cyclisations are determined by the reaction barriers between this local minimum and the biradical intermediates; that is, the top of these barriers also has to be characterised in order to compare the yields of different reaction courses. If no local minimum near to $T_1(S_0\,\text{geom})$ exists, the cyclisation process to the biradical intermediates will start immediately.

Experimentally acquired data indicate that the photochemical cyclisation takes place on the lowest-lying triplet surface. DFT is sufficiently accurate to describe triplet biradicals, which, unlike singlet biradicals, can be properly described by a single reference approach.[18] While we employed the unrestricted density functional approach for the triplet states, the restricted approach was used to describe the equilibrium geometry of the S_0 state of the reactants. The computed S^2-values for the triplet states varied between 2.0 and 2.03. To check DFT to some extent, computations were also performed with the BLYP and with the B3LYP[19, 20] functionals. Both functionals gave the same overall trends for the triplet surface. The main differences are found for the relative position of the triplet biradicals with respect to the reactant. In comparison with the BLYP functional, the B3LYP functional computes lower relative energy positions of the triplet biradical intermediates with respect to the reactants ($\approx 5\,\text{kcal mol}^{-1}$). A similar effect had already been found for the singlet biradicals of enyne–allenes, in which the BLYP functional predicted the singlet biradicals to be too high in energy[9e, 9f] by about the same amount in relation to high level MR–CI+Q computations. Consequently, we only discuss B3LYP data below. To study the influence of the AO basis set we performed test computations with the 6-31G(d), the 6-311G(d) and the 6-311G(d,p)[21] basis sets. These test calculations showed differences between the 6-31G(d) and 6-311G(d) basis sets, but only small alterations if p-polarisation functions on the hydrogen were added. Consequently, the 6-311G(d) basis set was employed for all computations. The geometries of all stationary points were optimised by use of analytical energy gradients with the density function approach, the B3LYP functional being employed in combination with the 6-311G(d) basis set. The influence of the nuclear motion and temperature effects were incorporated in the standard approach.[22] All calculations were performed by use of the Gaussian98 package[22] and the TurboMole program[23] package.

Results and Discussion

The results of this work are summarised in Figure 1, Figure 2 and Figure 3, which contain the reaction profiles computed for the model systems **1**–**3**. Some selected geometrical

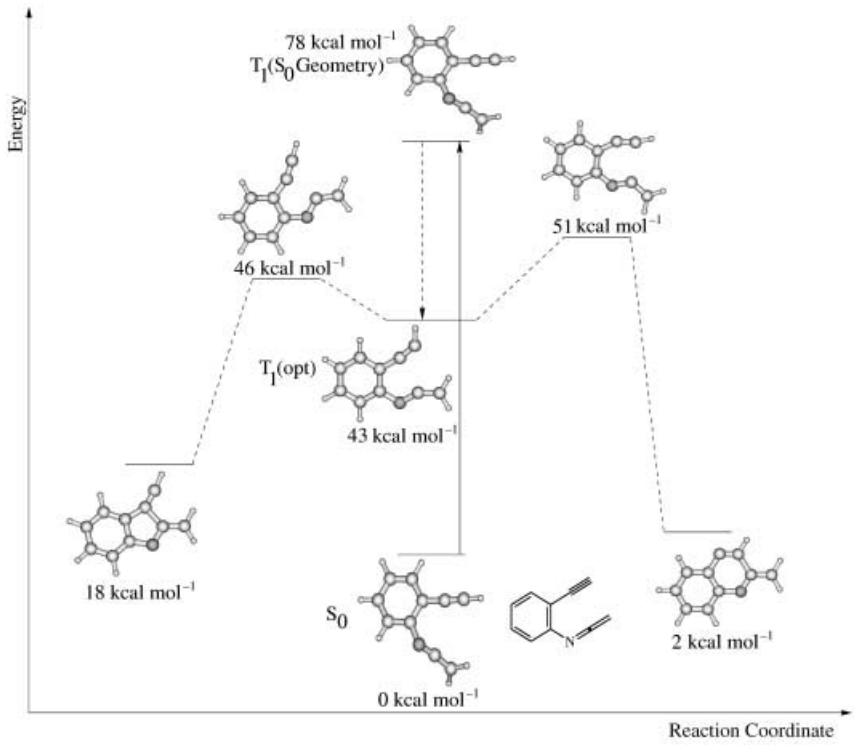

Figure 1. Energy profiles for the photochemical C^2-C^6 and C^2-C^7 cyclisation modes of **2** (see Scheme 3), which serves as a model compound for enyne – ketenimines. The sketches of the molecular geometries indicate the changes in the nuclear arrangement along the course of both cyclisation paths. In the middle of the figure, the reactant (S_0), the vertical excitation leading to $T_1(S_0$ geometry) and the local minimum to which the molecule relaxes after vertical excitation are given. On the left-hand side, the course of the C^2-C^6 cyclisation is depicted, while the path of the C^2-C^7 cyclisation is indicated on the right-hand side. All energies (kcal mol^{-1}) are given with respect to the reactant S_0. For more information see text.

parameter optimised for the stationary points can be taken from Table 1.

For an understanding of the differences found between the various model systems it is best to start the discussion with the enyne – ketenimine system **2**. As mentioned, the reaction profiles for both cyclisation modes are depicted in Figure 1, which also contains sketches of the alterations in the nuclear arrangement along the courses of both cyclisation paths and the relative energies of the various points with respect to the energy of the reactant. Optimised geometrical parameters for the stationary states can be taken from Table 1. The middle of Figure 1 indicates the reactant (S_0), the point on the triplet surface reached by a vertical excitation ($T_1(S_0$ geom)), and the local minimum to which the molecule relaxes after vertical excitation ($T_1(T_1$ geom)). The left-hand side shows the course of the C^2-C^6 cyclisation, while the path of the C^2-C^7 cyclisation is indicated on the right. The vertical excitation energy ($S_0 \rightarrow T_1(S_0$ geom)) is predicted to be about 78 kcal mol^{-1}. This value seems reasonable, since the use of toluene as triplet photosensitizer (triplet energy $E_T =$ 83 kcal mol^{-1}) already leads to conversion rates of 100 %.

From the point reached by the vertical excitation $T_1(S_0$ geom), the molecule relaxes to a local minimum ($T_1(T_1$ geom)), which is about 35 kcal mol^{-1} lower in energy than $T_1(S_0$ geom). The geometrical structure of $T_1(T_1$ geom) is also depicted in Figure 1. In this structure the ketenimine moiety is bent towards the C^6 centre (see Scheme 1 for the numbering of the various centres) and the terminal CH bond of the enyne group is also bent, so the five-membered ring is to some extent preformed. From this local minimum, both cyclisation routes possess quite small barriers, of about 3 kcal mol^{-1} for the C^2-C^6 cyclisation and 8 kcal mol^{-1} for the C^2-C^7 cyclisation. Thanks to the high excess energy of about 35 kcal mol^{-1} resulting from the relaxation from $T_1(S_0$ geom) to $T_1(T_1$ geom), both barriers can easily be surmounted. For a convenient comparison between our findings and experimental results, the data obtained by Schmittel et al.[1] are summarised in Scheme 4. From the reactants **4a** and **4b** they found conversions of about 100 %, but the yields of the products **5a** and **5b** were only 50 and 62 %, respectively. Molecular products connected with the biradical intermediate of the C^2-C^7 cyclisation could not be detected, but the formation of polymeric material was observed. Our findings can provide an explanation of the experimental results. In our interpretation, the biradical intermediate of the C^2-C^6 cyclisation, which is known to tend to intramolecular reactions, leads to the products **5a** or **5b** described by Schmittel et al. Because of the nature of the biradical intermediate of the C^2-C^7 cyclisation we expect that the polymeric material found experimentally arises from the C^2-C^7 cyclisation. This is supported by Scheme 4, which outlines the reactions of the compounds actually employed in the experimental work of Schmittel et al.[1] The biradical intermediate of the C^2-C^7 cyclisation should be quite stable,

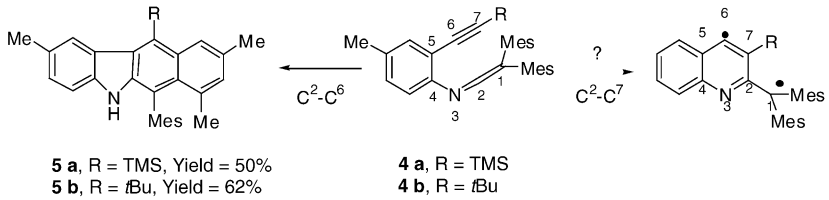

5 a, R = TMS, Yield = 50%
5 b, R = *t*Bu, Yield = 62%

4 a, R = TMS
4 b, R = *t*Bu

Scheme 4. Summary of the experimental results obtained by Schmittel et al.[1] for the photochemical cyclisation reaction of enyne – ketenimines.

Table 1. Selected optimised geometrical parameters for the stationary points depicted in Figure 1, Figure 2 and Figure 3. All data were obtained by the UB3LYP/6–311G* approach. The energy is given with respect to the reactants in the respective reaction. The angles are given in °, distances in Å. The corresponding geometrical arrangement is depicted for a simpler overview. The numeration of the centres can be taken from Scheme 3.

Equilibrium structure of the reactant, S_0 geom			
Compound	**1**	**2**	**3**
⟨(1–2–3)	168.6	174.3	174.6
⟨(2–3–4)	134.9	128.5	131.4
⟨(3–4–5)	123.6	122.7	125.7
⟨(4–5–6)	121.7	122.0	123.3
⟨(5–6–7)	178.5	177.8	175.7
R_{2-6}	2.98	3.08	3.04
R_{2-7}	3.43	3.59	3.51
Local minimum of the triplet surface, $T_1(T_1$ geom)			
Compound	**1**	**2**	**3**
⟨(1–2–3)	–	129.1	139.9
⟨(2–3–4)	–	127.3	127.4
⟨(3–4–5)	–	125.4	123.8
⟨(4–5–6)	–	123.0	122.5
⟨(5–6–7)	–	174.0	174.8
R_{2-6}	–	2.86	2.86
R_{2-7}	–	3.39	3.30
Triplet biradical obtained from the C^2-C^6 cyclisation, ($T_1(C^2-C^7)$			
Compound	**1**	**2**	**3**
⟨(1–2–7)	122.8	120.4	120.7
⟨(3–2–7)	120.5	121.4	117.2
⟨(4–3–2)	119.8	119.7	122.8
⟨(2–7–6)	117.7	116,7	118.1
⟨(7–6–5)	124.9	125.1	127.4
R_{2-7}	1.47	1.47	1.46
Triplet biradical obtained from the C^2-C^6 cyclisation $T_1(C^2-C^6)$.			
Compound	**1**	**2**	**3**
⟨(1–2–6)	124.1	126.1	125.4
⟨(3–2–6)	110.1	110.9	106.9
⟨(4–3–2)	107.0	107.1	110.2
⟨(2–6–7)	126.0	126.9	126.6
⟨(2–6–5)	103.4	103.1	105.7
R_{2-6}	1.52	1.51	1.51
R_{6-7}	1.32	1.32	1.32
Transition state of the C^2-C^6 cyclisation			
Compound	**1**	**2**	**3**
⟨(1–2–3)	–	132.8	141.1
⟨(5–6–7)	–	155.9	156.8
R_{2-6}	–	2.31	2.31
Transition state of the C^2-C^7 cyclisation			
Compound	**1**[a]	**2**	**3**
⟨(1–2–3)	123.7	127.8	134.3
⟨(5–6–7)	151.4	148.0	152.0
R_{2-7}	2.74	2.41	2.40

[a] See text.

since the radical centre at position 1 is strongly stabilised due to the two 2,4,6-$(CH_3)_3C_2H_6$ substituents. The strong stabilisation is not included in our model, but—as shown in Figure 1—the biradical intermediate of the C^2-C^7 cyclisation is similar to the reactant in energy even for hydrogen atoms as substituents, while the biradical intermediate of the C^2-C^6 cyclisation is about 18 kcal mol^{-1} higher in energy. Yields of **5a** and **5b** of more than 50% can be explained by the slightly lower barrier of the C^2-C^6 cyclisation and by the geometrical structure of local minima $T_1(T_1$ geom), which already resembles the transition state of the C^2-C^6 cyclisation.

The photochemical cyclisation of the enyne–carbodiimide systems has unexpected high yields of more than 90%. Consequently, our computations should predict remarkable differences between the triplet surfaces of the enyne–carbodiimide and of the enyne–ketenimine model system. This is indeed the case, as can be seen from Figure 2, which depicts the energy profiles computed for model compound **1.** It contains the main energy data for both cyclisation modes, together with sketches indicating the alterations in the nuclear arrangement along both reaction paths. Selected optimised geometrical parameters for the TS of the C^2-C^7 cyclisation can be taken from Table 1. Figure 2 is arranged as Figure 1, its centre indicating the reactant (S_0) and $T_1(S_0$ geom), and the reaction profiles of the C^2-C^6 and of the C^2-C^7 cyclisation depicted to the left- and the right-hand side, respectively. The computed vertical excitation energy of model compound **2** ($S_0 \rightarrow T_1(S_0$ geom)) is 78 kcal mol^{-1}, equal to that of the enyne–ketenimine (also 78 kcal mol^{-1}). In contrast to model compound **2**, however, a geometry optimisation starting at $T_1(S_0$ geom) leads directly to the biradical intermediate of the C^2-C^6 cyclisation, that is our computations predict that the photochemical cyclisation reaction of the C^2-C^6 cyclisation is barrierless and possesses an energy profile with a steadily descending energy. For the biradical intermediate of the C^2-C^6 cyclisation, our computations predict two possible isomers, differing in the orientation of the terminal NH group. Geometry optimisation starting from $T_1(S_0$ geom) leads to the isomer in which the hydrogen is oriented towards the second radical centre, located at C^7 (see Scheme 1 for the numbering of the centres). This shows that the cyclisation directly leads to that isomer that is already arranged for subsequent intramolecular reactions leading to the final products. The second isomer, in which the terminal NH bond is oriented away from the second radical centre, is more stable by about 2 kcal mol^{-1}, but the fact that our optimisation does not give the more stable isomer points to a barrier between the two isomers. In summary, the reaction profile of the C^2-C^6 cyclisation represents a perfect slide to the final products. It starts from the point reached by the vertical excitation ($T_1(S_0$ geom)) and proceeds with a steady negative energy gradient to the biradical intermediate of the C^2-C^6 cyclisation, which is perfectly arranged for the subsequent reactions. Clearly, this reaction profile perfectly explains the unexpectedly high yields found for enyne–carbodiimides since it to a large extent suppresses the C^2-C^7 cyclisation and further competing reactions.

The study of the rival C^2-C^7 cyclisation turned out to be complicated, because we could not find a reaction path from $T_1(S_0$ geom) to the biradical intermediate. To identify this path as a possible side-path of the C^2-C^6 cyclisation we examined the energy gradients obtained from the geometry optimisations performed along the C^2-C^6 cyclisation. As indicated in the geometrical structures outlined on the left-hand side of Figure 2, in the first stage of the cyclisation the carbodiimide moiety bends towards the enyne moiety. During

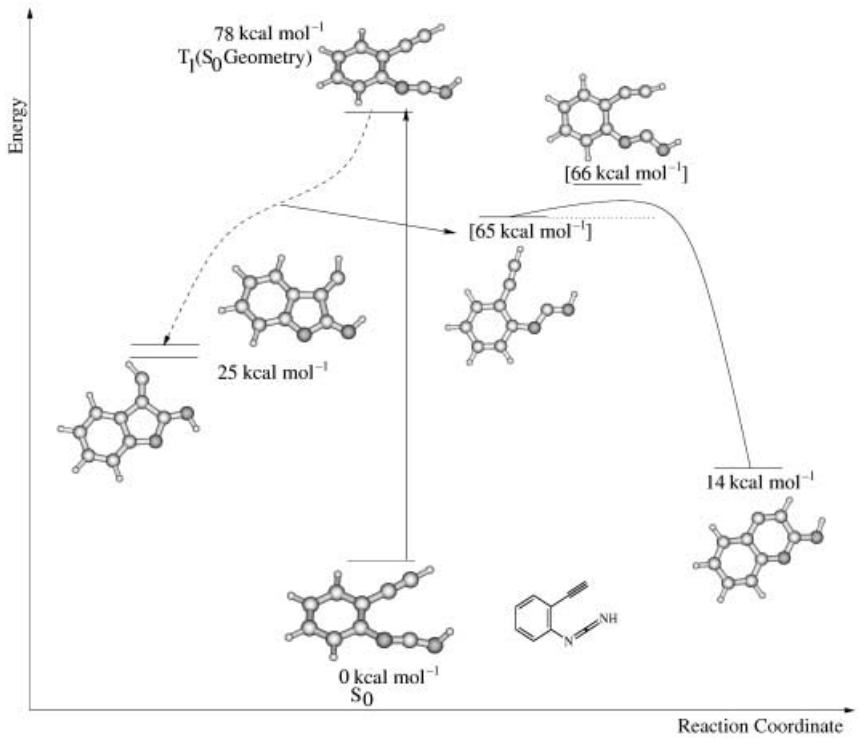

Figure 2. Energy profiles for the photochemical C^2-C^6 and C^2-C^7 cyclisation modes of **1** (see Scheme 3), which serves as a model compound for enyne – carbodiimides. All energies (kcal mol^{-1}) are given with respect to the reactant S_0. For more information see Figure 1 or text.

this stage the energy gradient of the triplet surface is quite high (i.e., the surface is steep). In the second stage, the surface becomes quite flat until in the last stage of the reaction the descent becomes steep again. In the last stage of the reaction the new bond between the C^2 and the C^6 centre is formed. In the flat region, the nuclei arrangements resemble the geometrical structure of the local minima $T_1(T_1$ geom) located for the enyne – ketenimine. By starting a transition state search for the C^2-C^7 cyclisation arbitrarily from the nuclei arrangement lying 65 kcal mol^{-1} above S_0 (depicted on the right-hand side), we were able to locate a path for the C^2-C^7 cyclisation. It possesses a transition state only about 1 kcal mol^{-1} higher in energy than the geometry from which we start the search. Nevertheless the transition state is about 12 kcal mol^{-1} below $T_1(S_0$ geom). This shows that the biradical intermediates of the C^2-C^7 cyclisation could also be reached without surmounting a high barrier, but that this cyclisation mode is suppressed due to the shape of the triplet surface, which clearly favours the C^2-C^6 cyclisation.

The reaction profiles computed for the enyne – allene model compound **3** (Figure 3) resemble that of the enyne – ketenimine **2**. Geometrical parameters optimised for the various stationary points can be taken from Table 1, while energy values are given in Figure 3. The geometry optimisation starting from $T_1(S_0$ geom) leads to a local minimum about 60 kcal mol^{-1} lower in energy. In addition, the geometry of this local minimum resembles the geometry found for the local minimum $T_1(T_1$ geom) of the enyne – ketenimine system. The allene moiety is bent towards the enyne moiety, but, unlike in the enyne – ketenimine system, the enyne moiety is still linear. From this local minimum, both cyclisations possess small barriers, computed to be about 3 kcal mol^{-1} for the C^2-C^6 cyclisation and 6 kcal mol^{-1} for the C^2-C^7

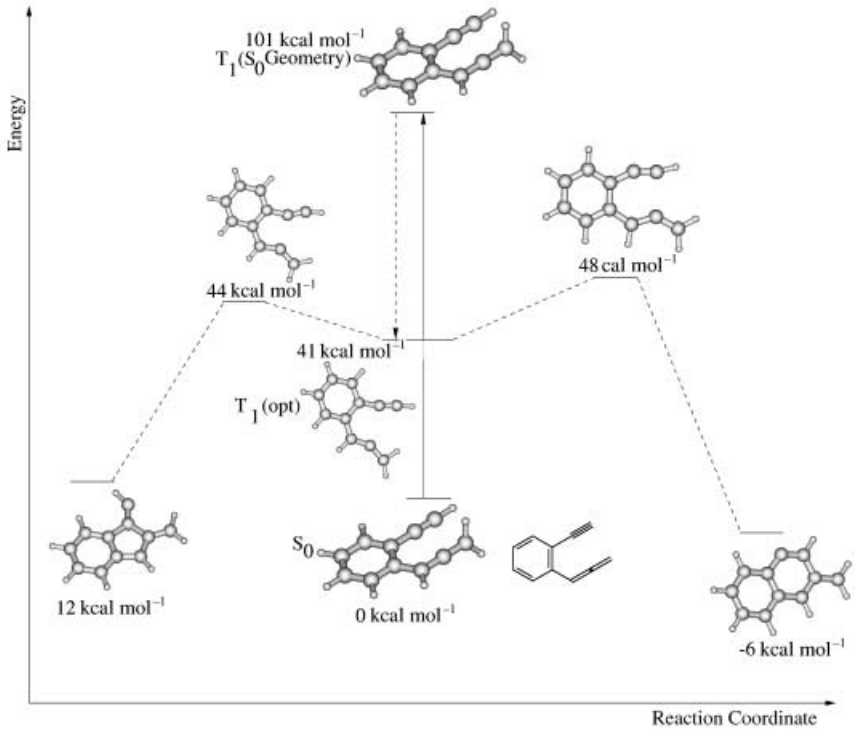

Figure 3. Energy profiles for the photochemical C^2-C^6 and C^2-C^7 cyclisation modes of **3** (see Scheme 3), which serves as a model compound for enyne – allenes. All energies (kcal mol^{-1}) are given with respect to the reactant S_0. For more information see Figure 1 or text.

cyclisation. While the shape of the triplet surface of the enyne–allene model compound **3** resembles the surface of the enyne–ketenimine system **2**, the vertical energies of the two compounds differ considerably. The vertical energy of **2** was computed to be about 78 kcal mol^{-1}, which lies within the range of the triplet photosensitizer employed by Schmittel et al. For the enyne–allene model system **3**, however, we calculate a much higher excitation energy of about 101 kcal mol^{-1}. Even if we take account of the error bar for the computed excitation energies and the possible influence of substituents that may lower the position of the triplet state it can be expected that the triplet energies of the employed triplet photosensitizer (50–80 kcal mol^{-1}) would not be sufficient to induce an effective $S_0 \rightarrow T_1$ excitation for enyne–allene compounds. As a consequence, no photoreaction can be observed.

Summary

Herein we discuss DFT calculations (B3LYP/6-311G* level of theory) performed to find an interpretation for the experimental results of Schmittel et al. concerning a highly efficient triplet analogue of the C^2-C^6 cyclisation of enyne–heteroallenes.[1] To shed some light on the reasons for the differences found between enyne–carbodiimide, enyne–ketenimines and enyne–allenes, we have computed the reaction profiles of the C^2-C^6 and C^2-C^7 cyclisations for the model compounds **1**–**3**, assuming that the reaction takes place on the lowest-lying triplet surfaces. Our results nicely explain the differences in the photochemical behaviour of enyne–heteroallenes and are able to account for the unexpectedly high efficiency of the enyne–carbodiimides. This can be reduced to the shape of the lowest-lying triplet surface, which—from a starting point reached by vertical excitation ($T_1(S_0$ geom))—represents a perfect slide to the biradical intermediates of the C^2-C^6 cyclisation. Furthermore, the obtained biradical intermediate possesses a perfect nuclear arrangement for subsequent reactions. The difference between enyne–carbodiimides and enyne–ketenimines originates from differences in the shapes of the corresponding triplet surfaces. Unlike the enyne–carbodiimides, which directly cyclise to the biradical intermediates after the vertical excitation, in the case of the enyne–ketenimines our computations predict a local minimum to which the molecule presumably relax after the vertical excitation. From this minimum, both cyclisation modes possess only small barriers, so that both routes can be taken. It has to be taken into account that the molecule possesses an excess energy of about 35 kcal mol^{-1} arising from the relaxation to this local minimum. We expect that for enyne–ketenimines the C^2-C^6 cyclisation leads to the products detected by Schmittel et al., while the C^2-C^7 cyclisation leads to the formation of polymeric material. While the computed excitation energy to the triplet state for enyne–carbodiimides and for enyne–ketenimines is below 80 kcal mol^{-1}, and thus in the range of the triplet photosensitizer employed by Schmittel et al., for the enyne–allene model compound **3** we calculate an excitation energy of more than 100 kcal mol^{-1}. We therefore expect that the enyne–allene compounds are outside the range of the triplet photosensitizer employed by Schmittel et al. Finally, the nice agreement between our results and the experimentally observed findings indicates that the underlying reasons for the differences in photochemical behaviour are related to alterations in the electronic structures of the parent systems, while substituents effects are less important for the cyclisation step itself.

Acknowledgements

The authors would like to thank Professor M. Schmittel for many fruitful discussions during the progress of this work. The investigation was supported in part by the Deutsche Forschungsgemeinschaft (DFG).

[1] M. Schmittel, D. Rodriguez, J.-P. Steffen, *Angew. Chem.* **2000**, *112*, 2236–2239; *Angew. Chem. Int. Ed.* **2000**, *39*, 2152–2155
[2] a) R. R. Jones, R. G. Bergman, *J. Am. Chem. Soc.* **1972**, 94, 660–661; b) R. G. Bergman, *Acc. Chem. Res.* **1973**, *6*, 25; c) T. P. Lockhart, P. B. Comita, R. G. Bergman, *J. Am. Chem. Soc.* **1981**, *103*, 4082–4890; d) T. P. Lockhart, R. G. Bergman, *J. Am. Chem. Soc.* **1981**, *103*, 4890; e) F. Ferri, R. Brückner, R. Herges, *New J. Chem.* ***1998***, *531–545*.
[3] a) N. Koga; K. Morokuma, *J. Am. Chem. Soc.* **1991**, *113*, 1907; b) P. G. Wenthold, R. R. Squires, *J. Am. Chem. Soc.* **1994**, *116*, 6401; c) R. Lindh, U. Ryde, M. Schütz, *Theor. Chim. Acta* **1997**, *97*, 203; d) C. J. Cramer, R. R. Squires, *Org. Lett.* **1999**, *1*, 215.
[4] a) J. Gräfenstein, A. M. Hjerpe, E. Kraka, D. Cremer, *J. Phys. Chem. A* **2000**, *104*, 1748–1761; b) E. Kraka, D. Cremer, *J. Mol. Structure., THEOCHEM* **2000**, *506*, 191; c) G. Jones, P. M. Warner, *J. Am. Chem. Soc.* **2001**, *123*, 2134–2145; d) M. Prall, A. Wittkopp, P. R. Schreiner, *J. Phys. Chem.* **2001**, *105*, 9265–9274; e) J. M. Galbraith, P. R. Schreiner, N. Harris, W. Wei, A. Wittkopp, S. Shaik, *Chem. Eur. J.* **2000**, *6*, 1446–1454; f) M. Prall, A. Wittkopp, A. A. Folkin, P. R. Schreiner, *J. Comput. Chem.* **2001**, *22*, 1605–1614; g) I. V. Alabugin, M. Manoharan, S. V. Kovalenko, *Org. Lett.* **2002**, *4*, 1119–1122.
[5] A. G. Myers, E. Y. Kuo, N. S. Finney, *J. Am. Chem. Soc.* **1989**, *111*, 8057–8059.
[6] R. Nagata, H. Yamanaka, E. Okazaki, I. Saito, *Tetrahedron Lett.* **1989**, *30*, 4995–4998.
[7] a) M. Schmittel, M. Keller, S. Kiau, M. Strittmatter, *Chem. Eur. J.* **1997**, *3*, 807–816; b) M. Schmittel, S. Kiau, M. Strittmatter, *Angew. Chem.* ***1996***, *108*, 1952–1954; *Angew. Chem. Int. Ed.* **1996**, *35*, 1843–1845; c) M. Schmittel, S. Kiau, T. Siebert, M. Strittmatter, *Tetrahedron Lett.* ***1996***, *37*, 7691–7694; d) M. Schmittel, M. Maywald, M. Strittmatter, *Synlett* ***1997***, 165–166; e) M. Schmittel, S. Kiau, *Liebigs Ann./Recueil* ***1997***, 733–736; f) M. Schmittel, K. Vollmann, M. Strittmatter, S. Kiau, *Tetrahedron Lett.* ***1996***, *37*, 999–1002; g) M. Schmittel, S. Kiau, *Tetrahedron Lett.* ***1995***, *36*, 4975–4978.
[8] a) T. Gillmann, T. Hülsen, W. Massa, S. Wocadlo, *Synlett* **1995**, 1257; b) J. G. Garcia, B. Ramos, L. M. Pratt, A. Rodriguez, *Tetrahedron Lett.* ***1995***, *36*, 7391.
[9] a) B. Engels, C. Lennartz, M. Hanrath, M. Schmittel, M. Strittmatter, *Angew. Chem.* **1998**, *110*, 2067–2070; *Angew. Chem. Int. Ed.* **1998**, *37*, 1960–1963; b) B. Engels, M. Hanrath, *J. Am. Chem. Soc.* **1998**, *120*, 6356–6361; c) B. Engels, M. Hanrath, C. Lennartz, *Comput. Chem.* **2001**, *11*, 15–38; d) P. W. Musch, B. Engels, *J. Am. Chem. Soc.* **2001**, *123*, 5557–5562; e) P. W. Musch, B. Engels, *Angew. Chem.* **2001**, *112*, 3951–3954; *Angew. Chem. Int. Ed.* **2001**, *40*, 3833–3836; f) P. W. Musch, C. Remenyi, H. Helten, B. Engels, *J. Am. Chem. Soc.* **2002**, *124*, 1823–1828.
[10] P. R. Schreiner, M. Prall, *J. Am. Chem. Soc.* **1999**, *121*, 8615–8627.
[11] a) M. Schmittel, J.-P. Steffen, B. Engels, C. Lennartz, M. Hanrath, *Angew. Chem.* **1998**, *110*, 2531–2533; *Angew. Chem. Int. Ed.* **1998**, *37*, 2371–2173; b) M. Schmittel, J.-P. Steffen, A. Wencesta, B. Engels, C. Lennartz, M. Hanrath, *Angew. Chem.* **1998**, *110*, 1633–1635; *Angew. Chem. Int. Ed.* **1998**, *37*, 1562–1564; b) L. D. Foland, J. O. Karlsson,

S. T. Perri, R. Schwabe, S. L. Xu, S. Patil, H. W. Moore, *J. Am. Chem. Soc.* **1989**, *111*, 975 – 989; c) H. W. Moore, B. R. Xerxa, *Chemtracts* **1992**, 273 – 313.

[12] a) K. K. Wang, *Chem. Rev.* **1996**, *96*, 207 – 222; b) J. W. Grisson, G. U. Gunawardena, D. Klingberg, D. Huang, *Tetrahedron* **1996**, *52*, 6453 – 6518

[13] a) *Enediyne Antibiotics as Antitumor Agents;* (Eds.; D. B. Borders,, T. W. Doyle), M. Dekker, New York, **1995**; b) Z. Xi, I. H. Glodberg, in *Comprehensive Natural Products Chemistry* (Eds.: D. H. R. Barton, K. Nakanishi), Pergamon, Oxford **1999**, Vol. 7, p. 553; c) G. B. Jones, J. M. Wright, G. Hynd, J. K. Wyatt, M. Yancisin, M. A. Brown, *Org. Lett.* **2000**, *2*, 1863; d) E. Kraka, D. Cremer, *J. Am. Chem. Soc.* **1999**, *122*, 8245 – 8264; b) M. E. Maier, *Synlett* **1995**, 13; e) *Neocarzinostatin: The Past, Present, and Future of an Anticancer Drug* (Eds.: H. Maeda, K. Edo, N. Ishida), Springer, New York, **1997**

[14] a) O. de Frutos, A. M. Echavarren, *Tetrahedron Lett.* ***1997***, *38*, 7941 – 7942. b) M. Alajarin, P. Molina, A. Vidal, *J. Nat. Prod.* ***1997***, *60*, 747 – 748.

[15] a) R. L. Funk, E. R. R. Young, R. M. Williams, M. F. Flanagan, T. L. Cecil, *J. Am. Chem. Soc.* **1996**, *118*, 3291 – 3292; b) A. Evenzahav, N. J. Turro, *J. Am. Chem. Soc.* **1998**, *120*, 1835 – 1841; c) T. Kaneko, M. Takahashi, M. Hirama, *Angew. Chem.* **1999**, *111*, 1347 – 1349; *Angew. Chem. Int. Ed.* **1999**, *38*, 1267 – 1268; d) J. Kagan, X. Wang, X. Chen, K. Y. Lau, I. V. Batac, R. W. Tuveson, J. B. Hudson, *J. Photochem. Photobiol. B. Biol.* **1993**, *21*, 135 – 142; e) G. B. Jones, J. M. Wright, G. Plourde, A. D. Purohit, J. K. Wyatt, G. Hynd, F. Fouad, *J. Am. Chem. Soc.* **2000**, *122*, 9872 – 9873; e) D. Ramkumar, M. Kalpana, B. Varghese, S. Sankararaman, M. N. Jagadeesh, J. J. Chandrasekhar, *Org. Chem.* **1996**, *61*, 2247; f) I. V. Alabugin, S. V. Kovalenko, *J. Am. Chem. Soc.* **2002**, *124*, 9052; g) H. E. Zimmermann, *J. Am. Chem. Soc.* **1973**, *95*, 3246; h) I. V. Alabugin, M. Manoharan, *J. Am. Chem. Soc.* **2003**, *125*, 4495.

[16] M. Schmittel, private communication.

[17] W. C. Agosta, P. Margaretha, *Acc. Chem. Res.* **1996**, *29*, 179 – 182.

[18] F. Jensen, *Introduction to Computational Chemistry*, Wiley, New York, **1999**.

[19] a) A. D. Becke, *Phys. Rev. A: At., Mol., Opt. Phys* **1988**, *38*, 3098 – 3100; b) A. D. Becke, *J. Chem. Phys.* **1993**, *98*, 1372 – 1377; c) A. D. Becke, *J. Chem. Phys.* **1993**, *98*, 5648 – 5652.

[20] C. Lee, W. Yang, R. G. Parr, *Phys. Rev. B* **1988**, *37*, 785 – 789.

[21] W. J. Hehre, R. Ditchfield, J. A. Pople, *J. Chem. Phys.* **1972**, *56*, 2257 – 2261.

[22] M. J. Frisch, G. W. Trucks, H. B. Schlegel, G. E. Scuseria, M. A. Robb, J. R. Cheeseman, V. G. Zakrevski, J. A. Montgomery, R. E. Stratmann, J. C. Burant, S. Dapprich, J. M. Millam, A. D. Daniels, K. N. Kudin, M. C. Strain, O. Farkas, J. Tomasi, V. Barone, M. Cossi, R. Cammi, B. Mennucci, C. Pomelli, A. Adamo, S. Clifford, J. Ochterski, G. A. Petersson, P. Y. Ayala, Q. Cui, K. Morokuma, D. K. Malick, A. D. Rabuck, K. Raghavachari, J. B. Foersman, J. Cioslowski, J. V. Ortiz, B. Stefanov, G. Liu, A. Liashenko, P. Piskorz, I. Komaromi, R. Gomperts, M. L. Martin, D. J. Fox, , T. Keith, M. A. Al-Laham, C. Y. Peng, A. Nanayakkara, C. Gonzalez, M. Challacombe, P. M. W. Gill, B. G. Johnson, W. Chen, M. W. Wong, J. L. Andres, M. Head-Gordon, E. S. Replogle, J. A. Pople, *Gaussian98*, Revision A.7, Gaussian, Inc., Pittsburgh, PA, **1998**.

[23] TURBOMOLE, R. Ahlrichs, M. Bär, H.-P. Baron, R. Bauernschmitt, M. Böcker, S. Ehrig, K. Eichkorn, S. Elliott, F. Haase, M. Häser, M. Horn, C. Huber, U. Huniar, M. Kattannek, C. Kölmel, M. Kollwitz, C. Ochsenfeld, H. Öhm, A. Schäfer, U. Schneider, O. Treutler, M. von Arnim, F. Weigend, P. Weis, H. Weiss, Quant. Chem. Group, University of Karlsruhe, Germany, since 1988.

Received: March 27, 2003 [F5001]

